Detection and extraction of endosulfan by metal nanoparticles

A. Sreekumaran Nair, Renjis T. Tom and T. Pradeep*

Department of Chemistry and Regional Sophisticated Instrumentation Centre, Indian Institute of Technology Madras, Chennai 600 036, India. E-mail: pradeep@iitm.ac.in; Fax: +91-44-2257 0509/0545

One of the most common pesticides in the developing world, endosulfan, can be detected in ppm levels using gold nanoparticles. Endosulfan adsorbs on the nanoparticle surface and upon interaction for a long time, the nanoparticles precipitate from the solution. Interaction with silver is weak, yet adsorption occurs leading to removal of endosulfan from the solution. A multilayer assembly of gold nanoparticles prepared on a glass substrate shows excellent spectrophotometric response suggesting potential applications.

Introduction

Endosulfan (6,7,8,9,10,10-hexachloro-1,5,5a,6,9,9a-hexahydro-6,9-methano-2,4,3-benzadioxathiepin-3-oxide) is one of the most stable pesticides known and has been detected in the environment throughout the world.[1] Its presence in the environment has been attributed to several health effects,[2] including genetic disorders. Aerial spraying of endosulfan in cashew nut plantations has been attributed to the large occurrence of birth defects in a village in southern India. Many of the long-term effects of exposure to this chemical have not been studied[1] and therefore, there are potential dangers to the exposed population. Due to its long environmental life span, it is necessary that proper detection and destruction methods are available in the affected regions. In view of these, we thought it important to investigate the possible use of metal nanoparticles in sensing and destroying endosulfan. We were prompted to look at this possibility on the basis of our earlier report on the catalytic destruction of halocarbons by metal nanoparticles[3a] as part of our research program on metal clusters.[3b] In this article, we show that endosulfan can be detected and can be selectively extracted by noble metal nanoparticles. The chemistry occurs in a wide concentration range of environmental significance and the processes can be used for field detection and may be scaled up for environmental decontamination, drinking water purification, *etc*. The chemical procedures involved are simple and can be adapted to the village environment making it a practical technology.

Experimental

All special chemicals used were from Aldrich. The experiment was conducted with gold and silver nanoparticles prepared using published procedures. Gold (silver) nanoparticles of 10–20 (60–80 nm) nm diameters were prepared by the citrate reduction route.[4] Briefly the method involves reducing 5×10^{-4} M Au^{3+} (Ag^+) by 1.2×10^{-3} M citrate in water by refluxing for 30 min. The cluster solution was wine red for gold and yellow for silver.[5] Stock solution of endosulfan was prepared in 2-propanol (as endosulfan solubility in water[6] is 3 ppm) and was diluted to the required concentration with the same solvent. The endosulfan solution was mixed with the citrate stabilized nanoparticle solution in water to get the reported concentration. Compositions of all the solutions in a set of studies were the same, except for endosulfan. In the dilute solution limit, the solutions were prepared with water itself and the effect was found to be the same. UV-visible spectra were recorded with a Perkin Elmer Lambda 25 spectrometer and FT-IR spectra were recorded with a Perkin Elmer

Spectrum One instrument using 5% (by weight) KBr pellets. Time dependent spectra were monitored in the cuvette itself without stirring. The nanoparticles did not precipitate after the reaction for a period of 9 h. In order to take IR spectra, the particles were precipitated by centrifugation at 3000 rpm for ½ h and the precipitate was washed with 2-propanol twice and air-dried. The particles were characterized by transmission electron microscopy (Philips CM12, 120 KeV) and powder X-ray diffraction (Shimadzu XD-D1 diffractometer with Cu Kα radiation, 30 kV, 20 mA).

Results and discussion

In Fig. 1, we show the change in the optical absorption spectrum of the nanoparticle solution upon exposure to endosulfan of different concentrations. The concentrations were 2, 10, 100 and 250 ppm, respectively and the spectra were recorded after 9 h of the addition of endosulfan. The plasmon absorption at 524 nm decreases in intensity after 3 h upon addition and an additional peak emerges at longer wavelengths. Dampening and the shift of the plasmon indicate adsorbate binding on the nanoparticle surface.[7] As the concentration of endosulfan increases, the red shift becomes more pronounced. The inset shows pictures of the nanoparticle solutions, 9 h after
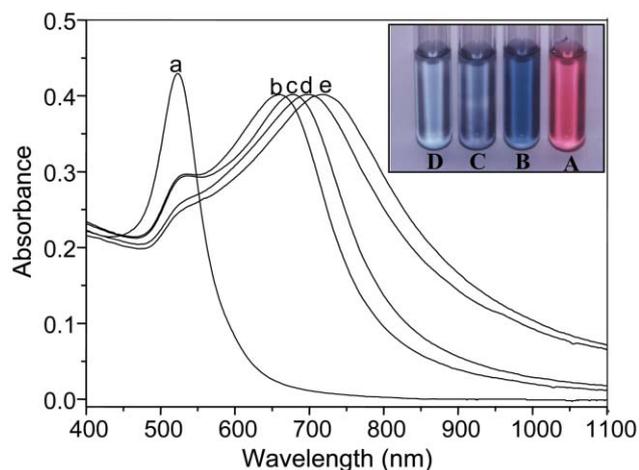

Fig. 1 UV-visible absorption spectrum of citrate stabilized gold nanoparticles (a) and the effect of exposure of endosulfan at various concentrations: (b) 2 ppm, (c) 10 ppm, (d) 100 ppm, and (e) 250 ppm. The spectra were recorded 9 h after exposure to endosulfan. The solutions have the same composition, except for endosulfan. A photograph of the solutions is shown in the inset. (A) Pure citrate stabilized nanoparticles; (B), (C) and (D) correspond to 2, 10 and 100 ppm, respectively.
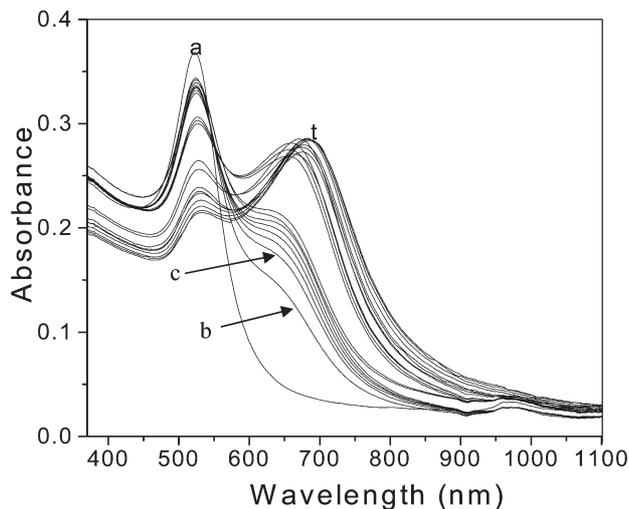
Fig. 2 Time dependence of the UV-visible absorption spectrum of citrate stabilized gold nanoparticles upon exposure of 10 ppm endosulfan. (a) Original nanoparticle solution, (b) 3 h after adding endosulfan solution, (c) to (t), at 20 min intervals thereafter.

the addition of 2 (B), 10 (C) and 100 (D) ppm of endosulfan. Intensity of color change is nearly quantitative and therefore, offers a colorimetric method for its detection. The response is better at low concentrations.

Fig. 2 represents the time dependent UV-visible spectra of gold nanoparticle solution upon exposure to 10 ppm endosulfan. Spectrum a represents absorption spectrum of pure citrate capped gold nanoparticles. The trace b was recorded after 3 h of the addition of endosulfan (composition of all solutions is the same). The peak at 524 nm decreases in intensity and a new peak emerges at longer wavelength (643 nm). Subsequent traces, (c–t) were recorded at 20 min intervals thereafter. As can be seen, with the passage of time, the new peak at longer wavelength emerges stronger in intensity accompanied by further red shift. The red shift in the plasmon can be attributed to adsorption of endosulfan on the surface of gold nanoparticles. After 9 h the solution becomes completely bluish and the material begins to settle down, possibly due to interparticle interaction. The residue can be removed by centrifugation.

Fig 3 presents the UV-visible spectra of silver nanoparticles after exposure to endosulfan of different concentrations. The spectra were recorded after 9 h of the addition of endosulfan. The spectra correspond to pure clusters (a) and after exposure to 2 ppm (b), 10 ppm (c), 100 ppm (d) and 250 ppm (e) of
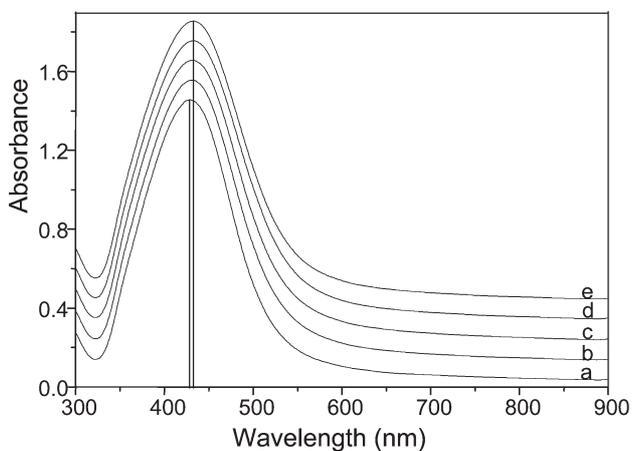

Fig. 3 UV-visible spectra of silver nanoparticles (a) after exposure to endosulfan of different concentrations. b, c, d and e are solutions having 2, 10, 100 and 250 ppm endosulfan. The spectra have been offset for clarity.
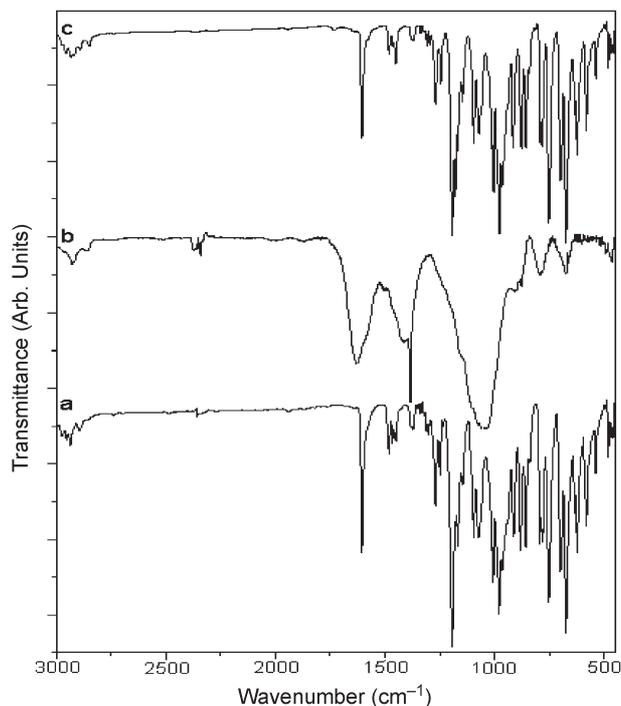
Fig. 4 Comparison of the infrared spectra of (a) pure endosulfan, residue after reaction with (b) gold and (c) silver. The reaction product with endosulfan (after 9 h) was separated by centrifugation and was washed with 2-propanol to remove free endosulfan, if any.

endosulfan, respectively. The shift in plasmon is not appreciable (~ 5 nm). The absorbance has been offset to show the shift in plasmon.

The precipitated bluish material was analyzed by FT-IR. Infrared spectrum of endosulfan is complex (Fig. 4a) in view of its reduced symmetry; but the characteristic absorptions[8] occur at 1600, 1192, 1270 and 750 cm^{-1} and can be assigned[9] to C=C, S=O, C–O and C–Cl stretches respectively. Upon adsorption on the gold nanoparticle, the features change substantially (Fig. 4b), almost all the features broaden, resulting in a complex spectrum. In contrast, the product obtained after reaction with silver nanoparticles gives a spectrum, almost identical to the parent endosulfan (Fig. 4c). There are some minor shifts in certain peak positions (such as 1192 cm^{-1}) indicative of weak interaction. In accordance with this reduced interaction, the UV-visible spectrum (Fig. 3) shows only a minor shift. However, the fact that endosulfan is bound to the silver particles and can be removed from the solution is significant. The separated particles can be suspended back into solution upon sonication. The feature at 1192 cm^{-1} shows splitting and the emergence of a new feature at 1179 cm^{-1} is evident, again due to adsorption at the surface. The C–Cl features do not change indicating negligible interaction of the Cl atoms with the surface. This interaction is distinctly stronger in gold; in addition to shifts this provides an additional channel for relaxation causing broadening of the features. It appears that the interaction is principally through sulfur.

In order to apply this chemistry to the field, we believe the better approach would be to use supported nanoparticle films. For a preliminary study, we prepared a gold nanoparticle film by layer-by-layer assembly on SnO$_2$ coated conducting glass plates. For this, we functionalized the glass surface with amino groups by exposing the cleaned glass surface to 3% solution of aminopropyltriethoxysilane for 1 h. After washing and drying at 100 °C for 1 h, the modified electrode was exposed to citrate-stabilized nanoparticles. This modified surface was then exposed to 1 mM solution of 1,6-hexane dithiol in 2-propanol for 5 h. After washing and drying again, the surface was exposed to citrate stabilized gold nanoparticle solution. The
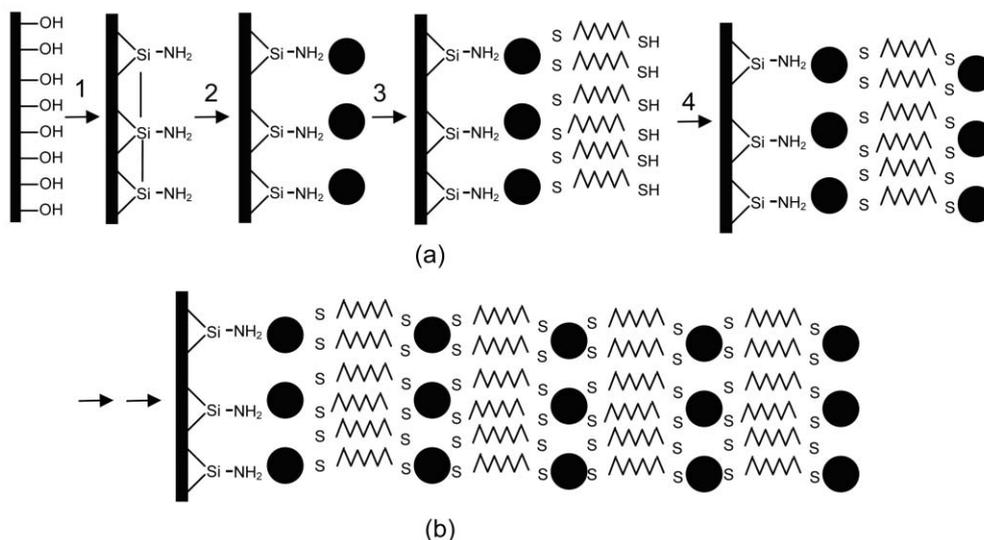
Scheme 1 (a) Schematic of the events involved in the formation of a metal cluster multilayer starting from a clean glass plate. Step 1 involves the preparation of aminofunctionalized glass substrate, step 2 leads to the adsorption of citrate stabilized gold clusters (black dots) on the surface, step 3 results in the adsorption of dithiol monolayers leading to partial substitution of citrate with thiolate and step 4 leads to further adsorption of the nanoparticles. By repeating 3 and 4, multilayers can be obtained. (b) Schematic of the multilayer used in this study.

processes were repeated to make five layers of gold nanoparticles. A schematic of the process is given in Scheme 1.

Absorption spectrum of the film taken in the transmission mode is shown in Fig. 5a. The nanoparticle absorption occurs at 525 nm. The side band occurring at 609 nm is due to the electronic interaction between the particles.[10] Note that this band occurs only after the formation of the second layer. Upon exposure of 10 ppm endosulfan solution for 10 h, the spectrum shifts to the red, the plasmon excitation is observed at 539 nm. The peak shifts by 14 nm. The film changes color visibly (from pale pink to light blue). Figs. 1, 2 and 5 suggest that the observed chemistry is reproducible. The enhancement of plasmon intensity is attributed to the intercalation of endosulfan into the bulk of the film leading to the partial substitution of thiolate linkages. Note that endosulfan binding is expected to be weaker than that with thiolate, resulting in increased surface electron density.

The chemicals involved in the synthesis of nanoparticles are commonly available, cheap and nontoxic and the chemistry involved in the preparation of nanoparticle solutions is simple, making this an immediately field adaptable method in rural communities.
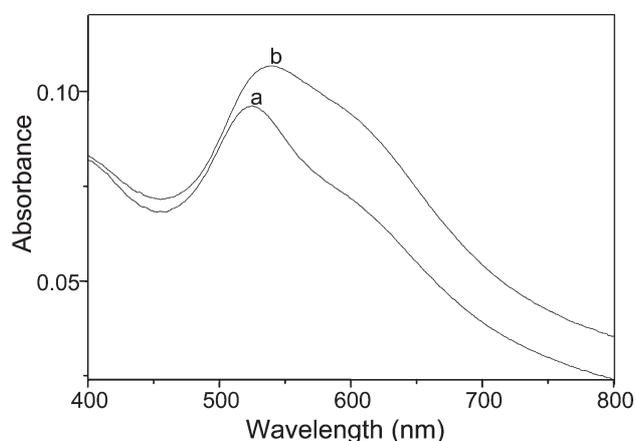
The chemistry described here is in general applicable to a range of halocarbons. With simple halocarbons such as CCl_4, complete mineralization occurs while with more complex halocarbons such as o-$C_6H_4Cl_2$, adsorption on the nanoparticle surface leading to a shift in the plasmon excitation is observed. We are currently pursuing the chemistry with a range of halocarbons.

In conclusion, we have demonstrated the use of metal nanoparticles in the detection of a common pesticide, endosulfan by spectrophotometry. The interaction of endosulfan with the nanoparticle surface leads to a shift in the surface plasmon resonance of the metal. The interaction is weak in the case of silver, yet adequate for the removal of endosulfan from solution. A multilayer assembly of gold nanoparticles on glass substrates is sensitive to endosulfan.

References

1 Toxicological profile of endosulfan prepared by the Agency for Toxic Substances and Disease Registry (ATSDR) (available at http://www.atsdr.cdc.gov/toxprofiles/tp41.html) provides detailed information.
2 There are 1200 reports on endosulfan since 1975 as per a search conducted using *http://www.webofscience.com*.
3 (*a*) A. Sreekumaran Nair and T. Pradeep, submitted; (*b*) N. Sandhyarani and T. Pradeep, *Int. Rev. Phys. Chem.*, in press; and the references cited therein.
4 J. Turkevich, P. L. Stevenson and J. Hillier, *Discuss. Faraday Soc.*, 1951, **11**, 55.
5 P. V. Kamat, M. Flumiani and G. V. Hartland, *J. Phys. Chem. B*, 1998, **102**, 3123.
6 H. Maier-Bode, *Properties, Effect, Residues, and Analytics of the Insecticide Endosulfan*, in *Residue Reviews*, 1968, vol. 22, pp. 10–44.
7 (*a*) F. X. Zhong, L. Han, L. B. Israel, J. G. Daras, M. M. Maye, N. K. Ly and C. J. Zhang, *Analyst.*, 2002, **127**, 462; (*b*) S. Link and M. A. El-Sayed, *Int. Rev. Phys. Chem.*, 2000, **19**, 409.
8 NIST Chemistry Web book available at *http://www.webbook.gov/chemistry*.
9 N. L. Alpert, W. E. Keiser and H. A. Szymanski, *IR Theory and Practice of Infrared Spectroscopy*, Plenum Press, New York, 1963.
10 B. Sadtler and A. Wei, *Chem. Commun.*, 2002, 1604.

Fig. 5 Demonstration of endosulfan sensing properties of gold nanoparticle coated electrode. Five layers of nanoparticles have been deposited on the electrode surface by self-assembly. The peak at 609 nm is due to inter-particle interaction. Note the red shift in the intensity of plasmon after the adsorption of endosulfan.